Lithology and Mineralogy Estimation from Matrix Density Utilizing Wireline Logs in Glauconitic Sandstone, Blackfoot Area, Alberta, Canada

Omar Mazen Derder

NEOSEIS TECHNOLOGY GROUP LTD., CALGARY, AB CANADA

ABSTRACT

The purpose of this work focuses on the estimation of lithological and mineralogical contents of rocks of the Glauconitic Sandstone Formation within Western Canadian Sedimentary Basin, Blackfoot area, Alberta, Canada. Gamma ray logs, neutron logs and density logs from oil wells were used to estimate and delineate the different lithologies, porosities and bulk densities at various depths for three wells in the same location.

The area studied consists in general of sandstone, shale and minerals such as siderite and pyrite. Three wells, named 1-8-23-23W4, 8-8-23-23W4 and 16-8-23-23W4 were chosen in order to quantify parameters needed to evaluate contents of rocks in the study wells.

Results from the log data demonstrate that the Glauconitic Formation contained predominately sandstone that was less dense than shale, and the matrix densities of the sandstone were higher than bulk densities. Matrix densities lie in the range between 2.4 g/cm3 and 3.4 g/cm3 with an average of 2.72 g/cm3 for the three wells, which is a comparable to established lithological and mineralogical standards of the Glauconitic Sandstone Formation.

The significance of the study is that in the absence of core data, the methods used in the work can assist in the identification and establishment the content of rocks, and in estimation the petrophysical properties such as porosity, permeability and fluid content. The results of this work consequently can be used in reservoir and basin analysis.

INTRODUCTION

The Blackfoot Field is located about 15 km southeast of the town of Strathmore, south-eastern Alberta in Canada (Figure 1). The target formation within the Blackfoot area is a Lower Cretaceous, Glauconitic Sand Formation (GSF). In the Blackfoot area, the Glauconitic Sandstone is encountered at a depth of about 1550 m and the valley-fill sediments are up to 45 m thick.

The Glauconitic Sandstone in this area is composed of a complex incised-valley system, which has eroded into regional Glauconitic deposits, removed the Ostracod Formation, and locally cut as deep as the Detrital Formation. It is subdivided into three phases of valley invasion. The three incised valleys are of different sand quality. The upper and lower incised valleys are the main reservoirs, the lower and upper members are made up of quartz sandstone, while the middle member is tight lithic sandstone. The lithic inside valley sand deposits are non-reservoir quality and act as permeability barrier between upper and lower incised valleys.

The Glauconitic consists of very fine to medium grained quartz sandstone in the eastern part, and quartz sandstone mixed with somewhat coarser lithic or sub-lithic sandstone in the western part of Alberta, and some siderite spherules are present in places. Interstitial clay and calcareous cement vary (Glass, 1997). The facies are composed of quartz and chert-rich sand with average porosity of 20% and average permeability of 750 mD.

The aim of this study is to identify and establish the lithological and mineralogical contents of rocks, and in the estimation of petrophysical parameters such as porosity, permeability and fluid content. The results of this work can be used in reservoir and basin analysis.

METHODOLOGY

Rock densities are among the least variable of all geophysical parameters. Most common rock types have densities in the range between 1.60 and 3.20 g/cm^3. The density of a rock is dependent on both its mineral composition and porosity. Variation in porosity is the main cause of density variation in sedimentary rocks; and the density of any particular rock type can be quite variable (Kearey et al., 2002).

Density is commonly determined by direct measurements on rock samples from core in the lab; it is necessary to measure several samples of each rock type to obtain a reliable mean density and variance. Core data is used to provide matrix densities for the particular intervals. However, the matrix composition may change and care must be taken within some lithological intervals. Analysis from some North Sea reservoirs shows that an error of 0.01 g/cm^3 in the matrix density gives an error of 0.5% in the calculated porosity (Bosch et al., 2002).

As well as these direct methods of density determination, there are several indirect (in-situ) methods that are used to yield valuable information for the rocks occurring at depth. Knowledge of rock density can aid in reservoir rock identification by lithology delineation, porosity determination from in-situ density measurements, and useful in the detection of gas-bearing formations (Rider, 2000).

Lithologies in the Glauconitic Sandstone in Blackfoot area are determined from core data and it was established that the rock matrix consist mainly of quartzose sandstone, lithic sandstone, calcareous shale and shale. Glauconitic Sandstone lithology indicates that there are additional mineral present such as siderite and pyrite.

Tamunobereton-ari et al. (2013) estimated the lithological and mineralogical contents of rocks in part of the Niger Delta Basin, using gamma ray, sonic and density logs from oil wells exploration. For the purpose of this work, gamma ray, neutron and density logs were used to determine the lithologic components of the formation of the area of the study, the porosity and the matrix densities.

Figure 1. Location map shows the study area and locations of wells available for this case study, in the Blackfoot area, Western Canadian Sedimentary Basin, Alberta, Canada. Alberta Map from Geological Atlas of the Western Canada Sedimentary Basin, 1994.

A manual interpretation of the lithology of the wells was undertaken using all the logs recorded through a regular approach. The gross lithology was verified and compared at the same depth to the gamma ray log. Gamma ray has been used as one of the independent shale indicators in the evaluation of GSF. Gamma ray logs are usually used to discriminate the shale from reservoir rock. The interpretation then continued through the other logs – resistivity, sonic, and density-neutron.

At depths where all the logs corroborated the same interpretation, the lithology was noted and then compared to cores. At depths where the lithology did not corroborate, a 'feedback' from one log to the next was done by way of log quality checking to correct the mismatch. The gross of thickness of Glauconitic sandstone in the studied wells 1-8-23-23W4, 8-8-23-23W4 and 16-8-23-23W4 are 28 m, 23 m and 28 m respectively (Figure 2).

Modern instruments for density log have two detectors (dual-detector density tool) situated at different spacing from the source, which allows borehole compensation to be applied. The density logging tool emits gamma ray from the source. The number of gamma rays arriving at the far detector is inversely proportional to the electron density of the rock (proportional to the actual rock density). Data from the closer detector is used to correct for borehole effect (Ellis and Singer, 2008).

The number density of electrons in a formation correlates with high bulk density. The electron density (the number of electrons per unit), $\mathbf{N_e}$, is the parameter used to describe the density of electrons in a formation. An electron density index, $\boldsymbol{\rho_e}$, is arbitrarily defined by:

$$\rho_e = 2N_e/N_A \tag{1}$$

Where $\mathbf{N_A}$ is Avogadro's number (6.02×10^{23} molecules/gmol). The number of atoms per unit volume, $\mathbf{N_a}$, and the number of electrons per unit volume, $\mathbf{N_e}$, can be expressed by:

$$N_a = N_A\,(\rho/A) \tag{2}$$

$$N_e = N_a Z = N_A\,(Z/A)\rho \tag{3}$$

Where $\boldsymbol{\rho}$ is the bulk density of the material in g/cm^3, $\mathbf{Z}$ is atomic number (no units), and $\mathbf{A}$ is the atomic weight (g/mole).

A linear relationship between the electron number density and the bulk density is observed, and the remaining parameters in the equation are either constant or a given element Z and A, or universally constant N. For most elements the value of Z/A is about 0.5, but there are several significant departures; hydrogen, for example, has a Z/A ratio of nearly 1. For this reason, it is convenient to define a new quantity, $\boldsymbol{\rho_e}$. Using the expression of $\mathbf{N_e}$ given by equation (3) gives:

$$\rho_e = 2\,\tfrac{Z}{A}\,\rho_b \tag{4}$$

Where $\boldsymbol{\rho_b}$ is the bulk density.

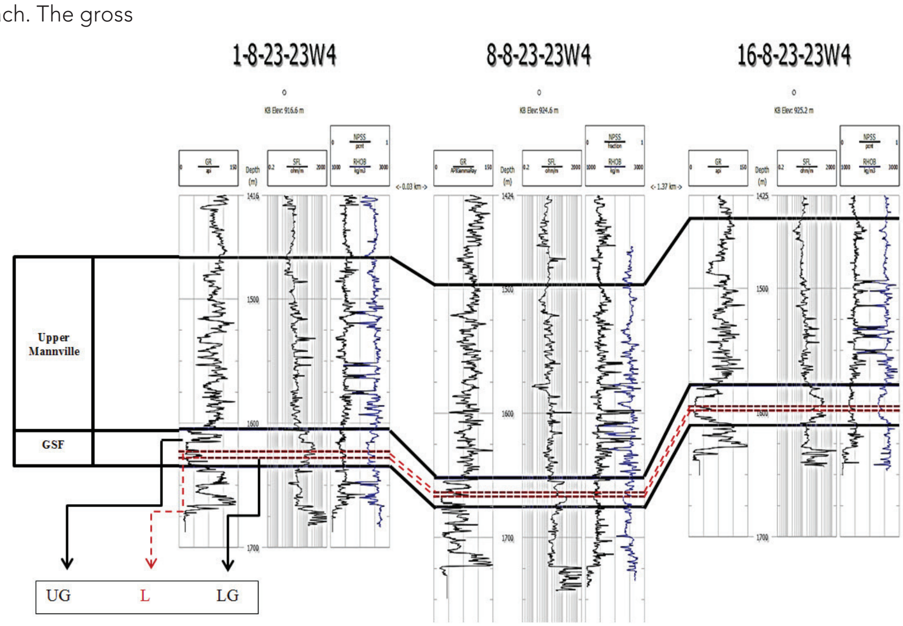

Figure 2. Well correlation of the Glauconitic Sandstone Formation. GSF (Glauconitic Sandstone Formation), UG (Upper Glauconitic), L (Lithic), LG (Lower Glauconitic).

Table 1 shows the value of **Z**, **A**, and **2(Z/A)** for the elements in the logging environment (Bassiouni, 1994, Ellis & Singer, 2008, Glover, 2013). Equation (4) can also be applied to rocks that contain more than one element. In this case the mean atomic number and mean atomic mass are used to substitute for Z and A respectively.

Table 1. The quantity **2(Z/A)** for elements present in the logging environment (Glover, 2013)

Element	A	Z	2(ZA)
H	1.008	1	1.9841
C	12.011	6	0.9991
O	16.000	8	1.0000
Na	22.99	11	0.9569
Mg	24.32	12	0.9868
Al	26.98	13	0.9637
Si	28.09	14	0.9968
S	32.07	16	0.9978
Cl	35.46	17	0.9588
K	39.10	19	0.9719
Ca	40.08	20	0.9980

Fluids densities are affected by dissolved solids, dissolved gases, compressibility, and temperature. These conditions cause density variations in ground fluid (Oberlander, 1988). The density of fresh water, salt water and oil is approximately 1.0 g/cm^3, 1.1 g/cm^3 and 0.9 g/cm^3 respectively. Dissolved solids and fluid compressibility increase density, whereas dissolution of gasses and thermal expansion caused by increased heat content reduce density.

Therefore in order to obtain accurate rock porosity measurements, it is important to obtain a fluid density data from samples of reservoir fluid or from Reservoir Fluid Temperature (RFT) analysis of mud filtrate (Tamunobereton-ari et al., 2013).

All the three porosity device (density, sonic and neutron) responses are affected by porosity, matrix, and fluid parameters. Most rocks have a wide range of densities. Therefore when used alone, it does not provide accurate identification of lithology. Sandstones, limestones and dolomites all have bulk density ranges that overlap each other and that of shale and density logs will not provide accurate data suitable for use in identifying lithology (Kearey et al., 2002; Bosch et al., 2002).

The value of matrix density depends on the lithology of the interval under study (Andrea et al., 1997). However, if there is a variable amount, it is important to choose the appropriate values of the matrix and fluid. The effect of errors in fluid and matrix density will effect on the accuracy of the porosity estimate. An uncertainty would be intolerable for making economic or engineering decisions.

Combination of three porosity tools if available, or at least combination of two porosity tools (density/neutron, sonic/neutron or density/sonic), will reduce the errors for the chosen lithology pairs among the three minerals (sandstone, dolomite and limestone) will have a negligible effect on the estimated porosity value.

Anomalously high or low density within a single lithology, or change in the character of the density log within a single lithology indicates that there are additional minerals present. Lower density will be observed when the lithology includes lignite, coal or increased organic matter in shale. In reverse, higher density will be observed when the lithology includes pyrite or siderite (Rider, 2000).

The bulk density $\boldsymbol{\rho_b}$ is overall gross or weight-average density of a unit of the formation (lithology and fluids). Because the tool's depth of investigation is shallow, it investigates the invaded zone. However, caution should be exercised when the density log is used in irregular borehole or in presence of gas/shale in the zone investigated by the density tool. In this case, the $\boldsymbol{\rho_b}$ of the formation is still undetermined (Bassiouni, 1994).

The $\boldsymbol{\rho_e}$ of fresh water mud filtrate, oil, and gas are small with those of matrices. The measured $\boldsymbol{\rho_e}$ is then affected slightly by porosity. $\boldsymbol{\rho_e}$, then is a good lithology indicator, especially when simple lithology (one dominant matrix) exists. The $\boldsymbol{\rho_e}$ value is used in combination with density to analyze two-mineral matrices and to determine porosity. It is combined with density and neutron porosity to analyze more complex lithologies.

Matrix densities can be determined from lithological and mineralogical characteristics of the rock body. Table 2 shows approximate bulk density $\boldsymbol{\rho_b}$ and electron density index $\boldsymbol{\rho_e}$ ranges for common elements, liquids and minerals. It can be determined that the $\boldsymbol{\rho_b}$ and $\boldsymbol{\rho_e}$ for a mixture of three major minerals (calcite, dolomite, and quartz) are identical.

However, for the case of water there is an 11% discrepancy between the two (due to anomalous Z/A value for H). Thus there will be an increasing discrepancy between $\boldsymbol{\rho_b}$ and the density tool response parameter $\boldsymbol{\rho_b}$, for increasing porosity. For this reason, to examine the effect of H, the density reading on logs has been calibrated to give precisely the bulk density of water-filled limestone. The relationship between the log reading **ρlog** and the $\boldsymbol{\rho_e}$ is:

$$\boldsymbol{\rho \log = 1.0704\rho_e - 0.188} \qquad (5)$$

Table 2. Density for various common rock types and minerals. Electron density $\boldsymbol{\rho_e} = \rho_b \times 2Z/A$

Rock / mineral types	Density (g/cm^3)	Electron Density (g/cm^3)
Anhydrite	2.29 – 3.0	2.957
Bituminous Coal	1.1 - 1.5	1.468
Clay	1.6 – 2.6	
Dolomite	2.8 - 2.9	2.864
Gypsum	2.3 - 2.8	2.372
Calcite	2.6 - 2.7	2.708
Pyrite	4.9 – 5.2	4.834
Quartz	2.5 - 2.7	2.650
Siderite	3.7 - 3.9	
Shale	2.4 - 2.8	2.646
Water	1	1.11
Salt Water	1.086	1.185
Oil	0.850	0.97

Composite logs containing gamma ray, neutron and density logs for three different wells were digitized at one meter depth intervals to obtain the raw well data for the determination of the parameters of interest. Lithologies are determined from core data and it was established that the rock matrix consists mainly of sandstone, shale with carbonaceous materials and siderite.

Accurate porosity determination is necessary for effective log interpretation. When the lithology, liquid-filled formation is known, representative porosity values can be derived from the reading of a porosity log. Log derived porosity values $\varnothing_D$ and $\varnothing_N$ can be expressed in general terms as:

$\varnothing_D$ or $\varnothing_N$ is f (matrix, total porosity, shale type and amount, type and amount of fluids in pore space. The neutron/density combination was used to compute for porosity as shown by equation (6) below (Bassiouni, 1994).

$$\rho_b = \rho_{ma} - (\rho_{ma} - \rho_f)f(\varnothing_N) \tag{6}$$

Where $\varnothing_N$ is the apparent porosity, ρ_f is the density of the fluid filling the pores, ρ_b is the bulk density of formation and ρ_{ma} is the matrix density. The density of the matrix ρ_{ma}, is also resolved as given by equation below:

$$\rho_{ma} = \frac{\rho_b - \varnothing * \rho_f}{1 - \varnothing} \tag{7}$$

Where $\varnothing$ is the true porosity.

For normally encountered formations, the value to be used for matrix density is generally between 2.65 and 2.87 g/cm^3, depending on lithology. For values of fluid density, it is necessary to know the type of fluid in the pores. The fluid density for hydrocarbon ranges from 0.2 to 0.8 g/cm^3. Salt-saturated water (NaCl) density may be as high as 1.2 g/cm^3, and with the presence of CaCl2, values even as great as 1.4 g/cm^3 may occur (Bosch et al., 2002).

The impact of the uncertainty in fluid density can be illustrated. For example, if the saturating brine is dense (1.4 g/cm^3) with calcite matrix, then the porosity uncertainty corresponding to the measured density of 2.5 g/cm^3 is 16%. On the other hand if the saturating fluid is low density (0.6 g/cm^3) then the calculated uncertainty for the porosity would be about 10%. It is fortunate that the uncertainty that can be tolerated in ρ_f is much greater than that of ρ_{ma}.

Equation (6) is used to compute for the matrix densities at different depths, saturated with different fluids (fresh water =1.0 g/cm^3, salt water = 1.1 g/cm^3, and oil = 0.9 g/cm^3) by substituting the appropriate values of the parameters in the equation. The three study wells are computed and the values presented by Tables 3, 4 and 5 respectively.

RESULTS

The digitized logs and the computed values are obtained for the three wells (1-8-23-23W4, 8-8-23-23W4 and 16-8-23-23W4); and presented by tables 3, 4 and 5 showing the selected depth intervals, GR values, porosities, bulk densities and the matrix densities for the Glauconitic formation saturated with different fluids. For the three wells, the relationship between the parameters shows that the shale from gamma ray is denser than sandstone (Figure 3). It is also evident that matrix densities are higher than the bulk densities.

For a given bulk density at a given depth of the formation interval; the matrix density, when the formation is assumed to be saturated with oil, is greater than when it is saturated with fresh water; and when saturated with the fresh water it is greater than when saturated with salt water. The result shows that aside from the mineral content of the solid rock materials, the porosity, the fluid type, and the volume of the fluid account for the magnitude of the dry solid matrix density of formation.

Graphical presentation of the plots of bulk densities against matrix densities shows bulk densities being lesser than matrix densities in all the wells at various depths (Figure 4). Ranges and averages of variation in percentage for matrix density from bulk density through the entire logged depth within the formation of the study wells that are saturated with different fluids are shown in Table 6.

The bulk densities and the matrix densities of the three wells at the same location are not the same and the average percentage variations of the matrix densities from bulk densities varied differently even at the same depth points.

To establish the reliability of the average percentage variations of the matrix densities from that of the bulk densities by taking water as a reference fluid, the average matrix densities variation of the same well when saturated with different fluids, we obtained an approximate uniformity for the three wells as shown in Table 7.

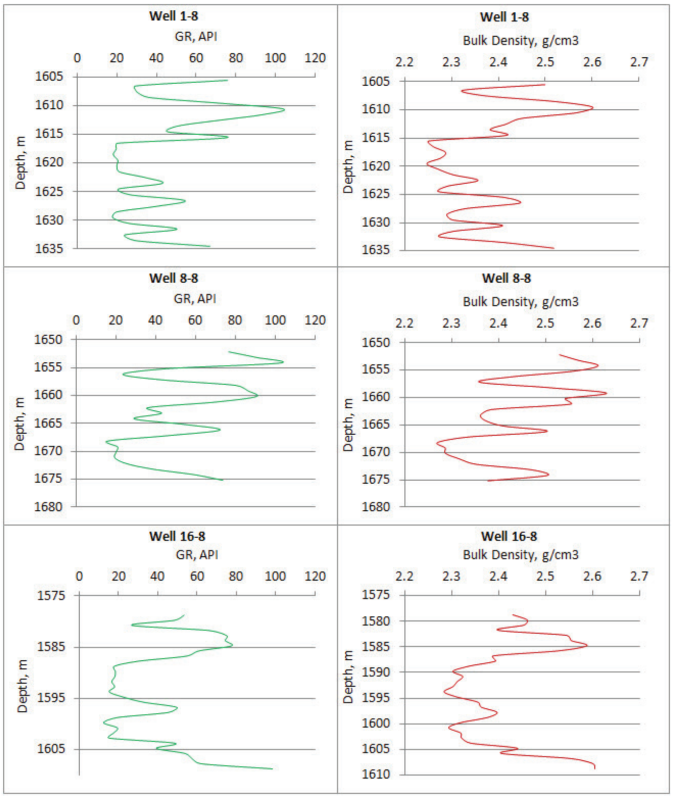

Figure 3. Shale interval is denser than sandstone for all wells in the study formation.

Table 3. Computed matrix densities for well 1-8-23-23W4

Depth (m)	GR (API)	Porosity %	Bulk Density (g/cm^3)	Matrix density (fresh water saturated formation) (g/cm^3)	Matrix density (salt water saturated formation) (g/cm^3)	Matrix density (oil saturated formation) (g/cm^3)
1606.5	29	17	2.32	2.60	2.58	2.62
1607.5	29	14	2.37	2.61	2.59	2.63
1608.5	36	15	2.52	2.80	2.79	2.82
1609.5	71	18	2.60	2.96	2.94	2.98
1610.5	103	19	2.56	2.95	2.93	2.97
1611.5	93	20	2.44	2.82	2.80	2.85
1612.5	71	19	2.41	2.75	2.73	2.77
1613.5	50	17	2.38	2.68	2.66	2.70
1614.5	45	17	2.41	2.71	2.69	2.73
1615.5	75	15	2.25	2.47	2.46	2.49
1616.5	20	11	2.26	2.41	2.40	2.42
1617.5	19	13	2.28	2.48	2.46	2.49
1618.5	18	15	2.27	2.50	2.49	2.52
1619.5	20	14	2.24	2.45	2.43	2.46
1620.5	19	13	2.27	2.47	2.45	2.49
1621.5	21	15	2.30	2.53	2.51	2.55
1622.5	34	20	2.35	2.69	2.67	2.72
1623.5	42	19	2.29	2.60	2.57	2.62
1624.5	20	16	2.27	2.51	2.49	2.53
1625.5	26	19	2.41	2.75	2.73	2.78
1626.5	54	22	2.44	2.87	2.84	2.90
1627.5	40	20	2.32	2.67	2.64	2.69
1628.5	19	18	2.29	2.57	2.55	2.60
1629.5	17	18	2.30	2.60	2.57	2.62
1630.5	26	18	2.40	2.72	2.70	2.74
1631.5	50	20	2.30	2.65	2.62	2.67
1632.5	23	19	2.27	2.58	2.55	2.60
1633.5	29	19	2.41	2.76	2.73	2.78
1634.5	67	19	2.51	2.87	2.85	2.90
Avg.	**40**	**17**	**2.36**	**2.66**	**2.63**	**2.68**

Table 4. Computed matrix densities for well 8-8-23-23W4

Depth (m)	GR (API)	Porosity %	Bulk Density (g/cm^3)	Matrix density (fresh water saturated formation) (g/cm^3)	Matrix density (salt water saturated formation) (g/cm^3)	Matrix density (oil saturated formation) (g/cm^3)
1652.178	77	21	2.53	2.94	2.91	2.96
1653.178	91	30	2.57	3.25	3.21	3.30
1654.178	103	32	2.61	3.36	3.32	3.41
1655.178	46	16	2.56	2.85	2.83	2.87
1656.178	24	18	2.43	2.74	2.72	2.76
1657.178	43	18	2.36	2.66	2.63	2.68
1658.178	80	20	2.51	2.88	2.86	2.91
1659.178	86	21	2.63	3.07	3.04	3.09
1660.178	91	22	2.54	2.99	2.96	3.02
1661.178	70	20	2.55	2.94	2.91	2.96
1662.178	36	18	2.38	2.70	2.67	2.72
1663.178	43	18	2.36	2.65	2.63	2.67
1664.178	29	14	2.37	2.60	2.58	2.62
1665.178	55	19	2.41	2.74	2.72	2.76
1666.178	72	19	2.50	2.85	2.83	2.88
1667.178	46	17	2.34	2.61	2.59	2.63
1668.178	16	14	2.27	2.48	2.46	2.49
1669.178	21	15	2.29	2.51	2.49	2.53
1670.178	20	19	2.29	2.58	2.56	2.60
1671.178	20	19	2.32	2.63	2.61	2.65
1672.178	25	20	2.35	2.69	2.67	2.72
1673.178	38	23	2.47	2.91	2.88	2.94
1674.178	59	24	2.50	2.97	2.94	3.00
1675.178	74	24	2.38	2.80	2.77	2.83
Avg.	**53**	**20**	**2.44**	**2.80**	**2.78**	**2.83**

Table 5. Computed matrix densities for well 16-8-23-23W4

Depth (m)	GR (API)	Porosity %	Bulk Density (g/cm^3)	Matrix density (fresh water saturated formation) (g/cm^3)	Matrix density (salt water saturated formation) (g/cm^3)	Matrix density (oil saturated formation) (g/cm^3)
1578.75	53	17	2.43	2.73	2.71	2.75
1579.75	49	17	2.46	2.75	2.73	2.77
1580.75	27	17	2.45	2.75	2.73	2.77
1581.75	66	19	2.40	2.72	2.70	2.74
1582.75	75	19	2.54	2.90	2.88	2.93
1583.75	74	21	2.55	2.98	2.95	3.00
1584.75	78	20	2.59	2.98	2.96	3.01
1585.75	61	20	2.53	2.91	2.89	2.94
1586.75	55	19	2.39	2.72	2.70	2.75
1587.75	30	16	2.39	2.67	2.65	2.69
1588.75	18	19	2.34	2.65	2.63	2.68
1589.75	18	17	2.30	2.56	2.54	2.58
1590.75	18	15	2.32	2.56	2.54	2.58
1591.75	17	15	2.31	2.55	2.53	2.57
1592.75	18	15	2.30	2.54	2.52	2.55
1593.75	15	15	2.28	2.52	2.50	2.53
1594.75	22	17	2.31	2.57	2.55	2.59
1595.75	33	18	2.36	2.65	2.63	2.67
1596.75	50	20	2.36	2.71	2.68	2.74
1597.75	45	21	2.40	2.77	2.74	2.79
1598.75	19	15	2.38	2.63	2.61	2.64
1599.75	12	15	2.32	2.56	2.54	2.57
1600.75	19	19	2.29	2.59	2.57	2.62
1601.75	18	21	2.32	2.67	2.64	2.70
1602.75	15	20	2.32	2.66	2.63	2.68
1603.75	49	20	2.34	2.67	2.64	2.69
1604.75	39	20	2.44	2.81	2.78	2.83
1605.75	54	22	2.41	2.81	2.78	2.84
1606.75	57	15	2.55	2.83	2.81	2.85
1607.75	62	19	2.60	2.98	2.95	3.00
1608.75	98	28	2.60	3.22	3.18	3.26
Avg.	**41**	**18**	**2.40**	**2.73**	**2.71**	**2.75**

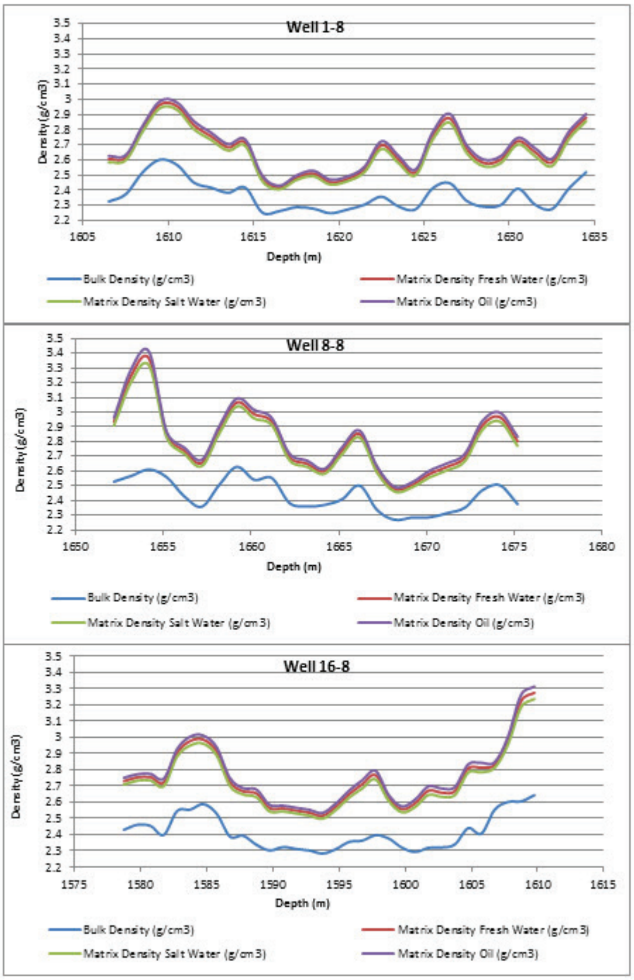

Figure 4: Plot of densities of Glauconitic Sandstone Formation with different fluid saturation versus bulk density for all study wells

Table 6: Variation of average matrix densities from average bulk densities of different fluids for the three wells

WELL	STATISTICS (%)		FLUID		
			Fresh Water	Salt Water	Oil
1-8	Average		11.16	10.43	11.87
	Range	Max	16.11	15.12	17.08
		Min	5.86	5.44	6.28
8-8	Average		13.16	12.37	13.93
	Range	Max	26.72	25.29	28.13
		Min	7.39	6.87	7.90
16-8	Average		11.84	11.10	12.57
	Range	Max	22.66	21.43	23.87
		Min	8.49	7.90	9.08

Table 7. Variation of average matrix densities of different fluids for the three wells from matrix saturated with fresh water for the three wells

Well	Fluid	Salt Water	Oil
1-8	Fresh Water	± 0.021	± 0.021
8-8		± 0.025	± 0.025
16-8		± 0.023	± 0.023

CONCLUSIONS

The Glauconitic Sandstone reservoir in these wells is heterogeneous consisting of a combination of clean sandstone and lithic sandstone. The wire-line logging data obtained was analyzed and computed values confirmed the lithologic sequence of the Glauconitic Sandstone Formation, which is quartz sandstone, glauconitic, siderite and calcareous cement.

The bulk densities of all three wells are lower than matrix densities. Also, the shale is denser than sandstone, and the type of the formation's fluid significantly influences the value of the bulk density. Matrix densities of the Glauconitic Sandstone Formation have a range from 2.40 gm/cm^3 to 3.40 gm/cm^3, which correlates to the density ranges of the matrix range for sandstone, shale and calcareous cement with the mineral constitute of siderite and pyrite.

The petrophysical data presented in this study can be used to identify, explore and extract by hydrocarbons in the Glauconitic Sandstone Formation for economic benefit. It is also hoped that the methods used in this study can be improved to determine other unknown petrophysical properties such as porosity, permeability, fluid contents etc. which are presently undetermined by this method of approach.

ACKNOWLEDGMENT

The Author is grateful to Dr. Rudi Meyer of University of Geoscience Department, University of Calgary who provided much of the background information concerning the Glauconitic Sandstone. My thanks also go to Dr. Ibrahim Inamah Abu of Petroleum Engineering Department, University of Calgary and Mr. Bill Hickman of NeoSeis Technology Group for the review of the manuscript. Thanks are also extended to the NeoSeis Technology Group for given NeoStrat® software and their support.

REFERENCES

Andrea, M.; Sams, M.S.; Worthington, M.H.; and Kings, M.S., 1997. Predicting Horizontal Velocities from Well Data, Geophysical Prospecting, 45: 593-609.

Bassiouni, Z. 1994. Theory, Measurement, and Interpretation of Well Logs, First Printing, Society of Petroleum Engineers, Richardson, TX.

Bosch, M.; Zamora, M; and Utama, W, 2002. Lithology Discrimination from Physical Rock Properties, Geophysics, 67: 573-581.

Ellis, D.V.; and Singer, J.M., 2008. Well Logging for Earth Scientists, 2nd ED. Published by Springer.

Geological Atlas of the Western Canada Sedimentary Basin, 1994, CSPG and AGS, Calgary, Alberta, Canada, Ch.19.

Glass, D.J., 1997. Lexicon of Canadian Stratigraphy. v4, Western Canada, ISBN 0-920230-23-7, Published by Flexys Systems.

Glover, P., 2013. Petrophysics MSc course Notes on Formation Density Log. PP. 121-138. http://www.scribd.com/doc/110298097/Petrophysics-P-glover-1#scribd.

Kearey, P.; Brooks, M.; and Hill, I., 2002. An Introduction to Geophysical Exploration, 3rd ED., T. J. International, Padstow, Cornwell.

Oberlander, P.L., 1989. Fluid Density and Gravitional Variations in Deep Boreholes and Their Effect on Fluid Potential. Ground Water, v. 27, No. 3.

Rider, M., 2000. The geological interpretation of well logs, Whittle publishing, Scotland. Printed by Inter-print Ltd., Malta.

Tamunobereton-ari, I.; Uko, E.D.; and Omubo-Pepple, V.B., 2013. Estimation of lithological and mineralogical contents of rocks from Matrix density in part of Niger Delta Basin Nigeria, using Well-log Data, Journal of Emerging Trends in Engineering and Applied Sciences (JETEAS), 4(6): 828-836.